

Published in final edited form as:

*Circ Cardiovasc Imaging*. 2011 March ; 4(2): 139–146. doi:10.1161/CIRCIMAGING.110.960229.

## Regional Thicknesses and Thickening of Compacted and Trabeculated Myocardial Layers of the Normal Left Ventricle Studied by Cardiovascular Magnetic Resonance

Dana K. Dawson, DM, MRCP, DPhil, Alicia M. Maceira, MD, Vimal J. Raj, MB, BS, FRCR, Catriona Graham, MSc, BSc(hons), Dudley J. Pennell, MD, FRCP, FACC, FESC, and Philip J. Kilner, MD, PhD

University of Aberdeen (D.K.D.), Aberdeen, UK; ERESA-Cardiac Imaging Unit (A.M.M.), Valencia, Spain; Leicester Royal Infirmary (V.J.R.), Leicester, UK; Clinical Research Facility (C.G.), Western General Hospital and University of Edinburgh, Edinburgh, UK; National Heart and Lung Institute, Imperial College, London, UK (D.J.P.); and Royal Brompton Hospital and the National Heart and Lung Institute, Imperial College, London, UK (P.J.K.).

### Abstract

**Background**—We used cardiovascular magnetic resonance (CMR) to study normal left ventricular (LV) trabeculation as a basis for differentiation from pathological noncompaction.

**Methods and Results**—The apparent end-diastolic (ED) and end-systolic (ES) thicknesses and thickening of trabeculated and compacted myocardial layers were measured in 120 volunteers using a consistent selection of basal, mid, and apical CMR short-axis slices. All had a visible trabeculated layer in 1 or more segments. The compacted but not the trabeculated layer was thicker in men than in women ( $P<0.01$  at ED and ES). When plotted against age, the trabeculated and compacted layer thicknesses demonstrated opposite changes: an increase of the compact layer after the fourth decade at both ED and ES ( $P<0.05$ ) but a decrease of the trabeculated layer. There was age-related preservation of total wall thickness at ED but an increase at ES ( $P<0.05$ ). The compacted layer thickened, whereas the trabeculated layer thinned with systole, but neither change differed between sexes. With age, the most trabeculated LV segments showed significantly greater systolic thinning of trabeculated layers and, conversely, greater thickening of the compact segments ( $P<0.05$ ). Total wall thickening is neither sex nor age dependent. There were no sex differences in the trabeculated/compacted ratio at ES or ED, but the ES trabeculated/compacted ratio was smaller in older (50 to 79 years) versus younger (20 to 49 years) groups ( $P<0.05$ ).

**Conclusions**—We demonstrated age- and sex-related morphometric differences in the apparent trabeculated and compacted layer thicknesses and systolic thinning of the visible trabeculated layer that contrasts with compacted myocardial wall thickening.

### Keywords

myocardium; trabeculae, myocardium, systolic thickening; isolated noncompaction of the ventricular myocardium; contractility

---

© 2011 American Heart Association, Inc.

Correspondence to Dana K. Dawson, DM, MRCP, DPhil, Royal Brompton Hospital, Sydney St, London SW3 6NP, UK. dana.dawson@abdn.ac.uk.

**Disclosures** None.

The online-only Data Supplement is available at <http://circimaging.ahajournals.org/cgi/content/full/CIRCIMAGING.110.960229/DC1>.

Comparisons of heart structure among the classes of living vertebrates together with studies of mammalian cardiogenesis suggest that a spongy, noncompact structure is the fundamental state of vertebrate ventricular myocardium. The process of compaction is an acquired characteristic in reptiles, birds, and mammals. In human embryonic development, a compact layer of myocardium appears and gains in relative thickness between the sixth and 12th week as ventricular septation is completed.<sup>1</sup> However, endocardial appearances on imaging or at postmortem inspection<sup>2</sup> show that mature human ventricles typically retain variable degrees of endocardial trabeculation,<sup>3</sup> with structural and mechanical properties that differ from those of the compact layer<sup>4</sup> and with considerable further variation between ventricular regions. This makes the definition of criteria for pathological left ventricular (LV) noncompaction (LVNC) challenging and controversial.<sup>5</sup> Because the current phenotypic definition of LVNC relies on the ratio of trabeculated/compacted myocardium, it is essential to have a detailed description of this ratio and its variability in the normal phenotype. In the current study, we used routine cardiovascular magnetic resonance (CMR) to visualize the segmental incidence, thicknesses, and thickening of the visible trabeculated and compacted myocardial layers in a prospectively recruited cohort of healthy volunteers.

## Methods

### Subjects

We recruited 120 normal volunteers (10 men and 10 women in 6 decile groups) aged 20 to 80 years. The baseline characteristics of this cohort have been published previously.<sup>6</sup> The study was approved by the Royal Brompton Local Research Ethics Committee, and all subjects gave informed consent.

### Imaging

All subjects underwent CMR imaging on a 1.5-T Siemens Sonata system. After localizers, 3 long-axis views and a complete short-axis stack of balanced, steady-state, free-precession cine images were acquired. Sequence parameters included repetition time of 3.2 ms; echo time, 1.6 ms; slice thickness, 7 mm; interslice gap, 3 mm; in-plane pixel size, 2.1×1.3 mm; and flip angle, 60°. Acquired pixels were routinely interpolated by the CMR system software during image reconstruction.

### Data Analysis

Data were analyzed with CMRTools (Imperial College; London, UK). A consistent selection of 3 designated short-axis slices was applied throughout. The basal slice measured was 2 cm down from the most basal short-axis slice located on the ventricular side of the atrioventricular junctions of both ventricles at end diastole (ED). The apical slice was 2 cm up from the most apical slice showing LV myocardium. The mid LV slice was equidistant in between. Manual measurements of the apparent ED and end-systolic (ES) thicknesses of the trabeculated and compacted layers in 16 of the standard 17 segments,<sup>7</sup> excluding the true apex, were made for each subject. A schematic presentation of the selection of slices corresponding to the basal, midventricular, and apical short-axis myocardial segmentation and assignment to walls is presented in Figure 1A. The boundary between compact and trabecular myocardium was chosen for each segment as the line outside which no trabeculations were apparent (Figure 1B). Review in cine mode can help to locate this boundary (online-only Data Supplement Movie 1). Because the trabecular layer could only rarely be described as having a uniform thickness in a particular segment, its thickness was measured from this boundary to the peak of the most prominent trabeculae in each segment. Measurements were performed by 2 independent, experienced observers for 6 patients to derive inter- and intraobserver variability. Wall thickening was calculated separately for the

trabecular and the compacted layers and for the total LV wall thickness by expressing the systolic increase of each apparent thickness as a percentage of its apparent ED thickness.

Statistical analysis was performed with MiniTab 15. Descriptive statistics are expressed as mean±SD (or SEM) if normally distributed and as median (first, third quartile) if nonparametric. Two-sample *t*, Mann-Whitney, 1-way ANOVA, and Kruskal-Wallis tests were used appropriately for parametric or nonparametrically distributed variables to determine differences with sex or age groups for each myocardial segment. Where ANOVAs were significant, linear regression was used to confirm trends. Variability was calculated as the difference divided by the mean of the 2 independently measured variables, expressed as mean±SD. Results were considered significant with a  $P<0.05$ .

## Results

### Segmental Incidence of Trabeculae

Figure 1 shows the incidence of an apparent trabecular layer in each segment at ED and ES. A trabecular layer was visible in 1 or more segments in all 120 volunteers. Trabeculae were prevalent in anterior and lateral segments at apical and midcavity levels but usually absent from septal segments. The apical lateral wall was the most commonly trabeculated territory, followed by the mid and apical anterior wall and midventricular lateral wall and less so by the inferior wall. No sex- or age-specific characteristic differences of trabecular distribution were identified. Trabeculae were consistently more apparent at ED than at ES. Intra- and interobserver variability is shown in Table 1.

### Trabecular and Compacted Layer Thicknesses and Their Variation With Sex and Age

Table 2 presents the mean individual thicknesses of the trabecular and compact layers and the full segmental wall thickness at ED and ES. The apical free wall was the only segment where the average trabeculated layer exceeded the compact layer thickness and only at ED.

There were significant sex differences when the thickness of the compacted layer was compared at both ES and ED ( $P<0.05$  for all segments), but no sex differences were found in trabecular layer thickness ( $P=NS$ ). There were corresponding differences between men and women in the total myocardial layer thickness for both phases of the cardiac cycle ( $P<0.05$  for all segments) (online-only Data Supplement Tables 1 and 2).

Figure 2 shows a representative age-related change in thickness of the compacted and trabecular layers at ED (shown here for the anterior wall segments), and Figure 3 illustrates corresponding findings at ES in the lateral wall. For all compacted myocardial segments, the pattern was similar, with a relatively higher thickness in the third decade of life followed by a slight decrease in thickness during the fourth decade and then progressive increase in each age decile. The differences across age groups in the compact layer thickness measured at both ED and ES were significant ( $P<0.05$  for all segments). Age-related differences also were found in the trabecular layer thickness with an opposite pattern of change compared to the compacted layer, but these differences did not reach significance for all examined segments ( $P<0.05$  for segments 1, 7, 13, and 16 at ED;  $P<0.05$  for segments 1, 5, 6, and 12, at ES; the remaining segments demonstrating only a trend, but  $P=NS$ ).

The age group-related changes in the compacted and trabecular layers contributed to a small, progressive increase in the total wall thickness measured at ES across age groups ( $P<0.05$  for all segments), but this difference was no longer apparent across all ED measurements ( $P<0.05$  only for segments 1, 7, 13, and 16;  $P=NS$  for all the rest). Figure 4A and 4B demonstrate the ES and ED total wall thickness changes with age for the anterior and lateral wall segments, respectively.

## Changes of the Trabecular and Compacted Layers During Systolic Contraction and Patterns of These Changes With Age

The apparent compacted layer thickened relatively uniformly by an average of  $73\pm 13\%$ . In contrast, the visible trabecular layer became thinner, generally making a negative contribution to total radial thickening, which averaged  $52\pm 13\%$  (individual segment analysis shown in Table 2). Neither the trabecular layer thinning nor the compact layer or total wall thickening were different between sexes in any segment ( $P=NS$ ) (online-only Data Supplement Table 3).

With regard to an age-related pattern in systolic changes, there were no significant differences in thickening across age groups for the total myocardial layer ( $P=NS$  for all segments). However, when the 2 components (trabecular and compacted layers) were examined separately, once again, an opposite pattern of change was observed. Figure 5 illustrates how the systolic thinning of the trabecular layer was progressively greater with age (statistically significant for segments 1, 6, 7, 11, 12, 15, and 16 [ $P<0.05$ ], whereas the remaining segments demonstrated only a trend in the same direction [ $P=NS$ ]). Conversely, as shown in Figure 5, the systolic thickening of the compacted layer was also progressively greater with age (statistically significant for segments 1, 6, 7, 11, 12, 15, and 16 [ $P<0.05$ ], whereas the remaining segments demonstrated only a trend that did not reach statistical significance). The segments where the age-related patterns of thickening and thinning were significant were the most trabeculated segments.

### The Trabecular/Compacted Layer Ratio and Its Changes With Cardiac Cycle and Age

The ratio between the apparent trabecular and compacted layers changed markedly through systole and diastole. At ED, the ratio was  $<1$  in all segments but the apical free wall. Of note, 64% of the normal volunteers had an apical free wall trabecular layer at least as thick as the compacted layer; 4 volunteers had an ED trabecular/compacted ratio  $>2$ , with 1 being  $>2.3$  (the highest trabecular/compacted ratio recorded in the cohort across all segments was 3) (Table 2). At ES, the ratio was  $<0.5$  in all segments with the exception of the apical free wall. Figure 6A shows the trabecular/compacted ratio for all segments. There were no sex differences when the trabecular/compacted ratio was compared at either ES or ED (online-only Data Supplement Tables 1 and 2). There were no age-related trends in the trabecular/compacted ratio at ED ( $P=NS$ ; graphs not shown). However, the trabecular/compacted ratio at ES was significantly smaller in the older groups (50 to 79 years) versus the younger groups (20 to 49 years), with  $P<0.05$  for all trabeculated segments (Figure 6B).

### Papillary Muscles and False Tendons

Papillary muscle heads were seen during both diastole and systole: minimum-maximum number of heads for the antero-lateral and posteromedial, respectively, were 0 to 4 and 0 to 3 at the basal level, 0 to 4 and 0 to 5 at the midventricular level, and 0 to 4 and 0 to 3 at the apical level. There were 14 false tendons, most of which were located at the basal LV level and in the anterior wall.

## Discussion

In the current study, we used CMR to determine the segmental incidence of a trabeculated layer and the apparent thickness and thickening of the trabecular, compacted, and total myocardial layers of the LVs of a prospectively recruited cohort of healthy volunteers. The main and novel findings of this study are as follows: (1) the prevalence and extent of trabeculated subendocardial regions in healthy individuals, (2) the apparent systolic thinning of the trabeculated layer in contrast to the marked thickening of the compacted layer during

contraction, and (3) specific age- and sex-related differences in the absolute and proportional thicknesses of these layers at ES and ED.

We chose to make linear measurements in routine short-axis CMR cines for several reasons. This approach is practical for retrospective analysis of routinely acquired CMR studies and lends itself to segmental analysis; further, the measurements can be compared directly with previously proposed echocardiographic criteria for LVNC.<sup>2,8</sup> We also believe that the orientation of the short-axis slices is preferable to long axis for technical reasons. Because the orientation of LV trabeculations tends to be predominantly longitudinal, CMR short-axis cines seemed more suitable for distinguishing the trabeculated from the compacted layers than the long-axis cines, as studied previously.<sup>9</sup> Because of the elongated shape of voxels constituting a cine image, short-axis images should be less prone to blurring of boundaries due to partial volume averaging.<sup>10</sup> However, disadvantages of short-axis slices include systolic through-plane myocardial movement, particularly relative to the basal slices, and the varying number of slices needed to cover ventricles of different sizes. For the latter reason, a consistent approach of slice selection was applied, regardless of ventricular size.

The compacted myocardial layer was consistently thicker across all segments in men than in women, and this relative difference was maintained throughout the cardiac cycle. The compacted myocardial layer was slightly thicker during the third decade of life; a slight decrease in thickness was observed during the fourth decade, after which it progressively increased until the eighth decade. These patterns suggestive of exercise conditioning/deconditioning at identical time points also were suggested by the Framingham cohort analysis.<sup>11</sup> The trabecular layer measurements showed an opposite trend for change with age. Because it is unlikely that trabeculae would continue to compact in adult life, the obvious explanation of our results is that these changes are due to age-related trabecular physiological hypertrophy. Because of hypertrophy, the interstices between the more epicardial trabeculae may become excluded, this region then appearing and being measured as compacted. However, no significant changes in the total myocardial layer thickness at ED were detected with increasing age, which suggests that the true compacted layer may remain relatively unchanged over time. These results are consistent with our previous results<sup>6</sup> and with those of others<sup>12</sup> who found no change with age in total LV mass measured from ED frames. These findings also can be reconciled with previous echocardiography studies that used LV wall thicknesses to derive changes in LV mass over time and concluded that there was a temporal increase in LV mass with age.<sup>13,14</sup> Because of the narrow ultrasound beam thickness (<5 mm) and noise, fine structures of various curvature and orientation, such as trabeculations, are less well resolved by the spatial resolution of 2D transthoracic echocardiography, and it is most likely that the perceived endocardial border on native echocardiography images was equivalent to our interpretation of apparent compacted layer boundary. This assumption is supported by the finding of larger ED volumes when LV opacification contrast agents were used versus smaller ED volumes resulting from native echocardiography images.<sup>15</sup> The age-related hypertrophy of the trabecular layer after the fourth decade translating into a progressively thicker effective compacted layer may be a necessary adaptation to maintain a constant myocardial wall stress, consistent with previously described age-related increases in both systolic and diastolic blood pressure after the fourth decade in healthy volunteers.<sup>16</sup> The concept of trabecular layer hypertrophy as a physiological phenomenon and the biphasic pattern of this hypertrophy have not been known to date.

With the systolic thickening and approximation of individual trabeculations, the apparent boundary between trabecular and compacted layers may shift relative to actual myocardial structures as visible interstices are eliminated. Part of the diastolic trabeculated layer may thus appear compact at ES, accounting in part for the apparent systolic thinning of the

trabeculated layer and the relatively high measurements made from CMR cine images of the apparent thickening of the compacted layer, which exceeded previously reported measurements of axially directed strain based on CMR myocardial tagging.<sup>17</sup> The subendocardial myocytes are predominantly longitudinally orientated. They must, individually, thicken in cross-section as they contract if they maintain their volume, in spite of the fact that the endocardial circumference is forced by the contraction of the more circularly oriented midmyocardial layers to diminish in systole.<sup>18</sup> This points to the potential mechanical advantage in the endocardium of a trabeculated rather than a compacted myocardial structure. With interstices between, not only the systolic thickening of myocytes, but also the circumferential shortening of the endocardium can be accommodated by the exclusion of intervening blood.

This interpretation is potentially relevant to the issue of diagnosing pathological LVNC in the presence of dilated cardiomyopathy.<sup>19</sup> An abnormally high trabeculated relative to compacted myocardial layer thickness at least in part may be a result and not necessarily a cause of dilatation. The global stretching of the dilated ventricular wall is likely to be associated with greater-than-normal separation of the trabeculations from one another and possibly from the abnormally thin compacted myocardial layer. Furthermore, the excessive wall tension relative to transmural pressure of a dilated heart tends, according to LaPlace law, to result in pathological hypertrophy, presumably of trabecular as well as of compacted myocardium. These effects would shift the ratio of visibly trabeculated to compacted myocardial thickness toward apparently noncompacted in any cardiomyopathy that results in global dilatation.

Finally, there were no significant changes related to either sex or age when the ratio of trabecular/compacted myocardium was examined at ED. Importantly, a ratio  $<1$  in all segments except the apical lateral wall appears to characterize the human volunteer cohort; this may have important implications in defining segmental LVNC. The trabecular/compacted ratio was significantly greater at ES in the young age groups compared to the older ones, which may have implications for the choice of cardiac phase<sup>2,8,9</sup> for discriminating normal from noncompacted LVs. The differentiation may be easier in segments with abundant rather than sparse trabecular preservation.

### Study Limitations

Cardiac CT could have offered better spatial resolution and isotropic voxel size than CMR. However, even with modern protocols, the radiation dose involved could not be justified in the case of volunteers. Because of the same spatial resolution constraints, we could not include segment 17 in our analysis.

### Conclusions

These results give novel insight into the prevalence, segmental distribution, dynamics, and likely functional role of a trabecular myocardial layer. We demonstrate for the first time, to our knowledge, age- and sex-related morphometric differences in the apparent trabecular and compacted layer thicknesses, which in turn contribute differently to the total wall thickening.

### Supplementary Material

Refer to Web version on PubMed Central for supplementary material.

## Acknowledgments

**Sources of Funding** Dr Dawson was the recipient of the van Geest Advanced Imaging Fellowship (UK). Dr Kilner is supported by the British Heart Foundation. The study was supported by the National Institutes of Health Research Cardiovascular Biomedical Research Unit at the Royal Brompton and Harefield NHS Foundation Trust and Imperial College.

## References

1. Wessels A, Sedmera D. Developmental anatomy of the heart: a tale of mice and man. *Physiol Genomics*. 2003; 15:165–176. [PubMed: 14612588]
2. Jenni R, Oechslin E, Schneider J, Attenhofer, Jost C, Kaufmann PA. Echocardiographic and pathoanatomical characteristics of isolated left ventricular non-compaction: a step towards classification as a distinct cardiomyopathy. *Heart*. 2001; 86:666–671. [PubMed: 11711464]
3. Weinsaft JW, Cham MD, Janik M, Min JK, Henschke CI, Yankelevitz DF, Devereux RB. Left ventricular papillary muscles and trabeculae are significant determinants of cardiac MRI volumetric measurements: effects on clinical standards in patients with advanced systolic dysfunction. *Int J Cardiol*. 2008; 126:359–365. [PubMed: 17698216]
4. Damon BJ, Remond MC, Bigelow MR, Trusk TC, Xie W, Perucchio R, Sedmera D, Denslow S, Thompson RP. Patterns of muscular strain in the embryonic heart wall. *Dev Dyn*. 2009; 238:1535–1546. [PubMed: 19418446]
5. Kohli SK, Pantazis AA, Shah JS, Adeyemi B, Jackson G, McKenna WJ, Sharma S, Elliott PM. Diagnosis of left-ventricular non-compaction in patients with left-ventricular systolic dysfunction: time for a reappraisal of diagnostic criteria? *Eur Heart J*. 2008; 29:89–95. [PubMed: 17993472]
6. Maceira AM, Prasad SK, Khan M, Pennell DJ. Normalized left ventricular systolic and diastolic function by steady state free precession cardiovascular magnetic resonance. *J Cardiovasc Magn Reson*. 2006; 8:417–426. [PubMed: 16755827]
7. Cerqueira MD, Weissman NJ, Dilsizian V, Jacobs AK, Kaul S, Laskey WK, Pennell DJ, Rumberger JA, Ryan T, Verani MS. Standardized myocardial segmentation and nomenclature for tomographic imaging of the heart: a statement for healthcare professionals from the Cardiac Imaging Committee of the Council on Clinical Cardiology of the American Heart Association. *Circulation*. 2002; 105:539–542. [PubMed: 11815441]
8. Chin TK, Perloff JK, Williams RG, Jue K, Mohrmann R. Isolated non-compaction of left ventricular myocardium. A study of eight cases. *Circulation*. 1990; 82:507–513. [PubMed: 2372897]
9. Petersen, Steffen E, Selvanayagam JB, Wiesmann F, Robson MD, Francis JM, Anderson RH, Watkins H, Neubauer S. Left ventricular non-compaction: insights from cardiovascular magnetic resonance imaging. *J Am Coll Cardiol*. 2005; 46:101–105. [PubMed: 15992642]
10. Chan KM, Wage R, Symmonds K, Rahman-Haley S, Mohiaddin RH, Firmin DN, Pepper JR, Pennell DJ, Kilner PJ. Towards comprehensive assessment of mitral regurgitation using cardiovascular magnetic resonance. *J Cardiovasc Magn Reson*. 2008; 10:61. [PubMed: 19102740]
11. Savage DD, Levy D, Dannenberg AL, Garrison RJ, Castelli WP. Association of echocardiographic left ventricular mass with body size, blood pressure and physical activity (the Framingham Study). *Am J Cardiol*. 1990; 65:371–376. [PubMed: 2137280]
12. Sandstede J, Lipke C, Beer M, Hofmann S, Pabst T, Kenn W, Neubauer S, Hahn D. Age- and gender-specific differences in left and right ventricular cardiac function and mass determined by cine magnetic resonance imaging. *Eur Radiol*. 2000; 10:438–442. [PubMed: 10756992]
13. Shub C, Klein AL, Zachariah PK, Bailey KR, Tajik AJ. Determination of left ventricular mass by echocardiography in a normal population: effect of age and sex in addition to body size. *Mayo Clin Proc*. 1994; 69:205–211. [PubMed: 8133657]
14. Gerstenblith G, Frederiksen J, Yin FC, Fortuin NJ, Lakatta EG, Weisfeldt ML. Echocardiographic assessment of a normal adult aging population. *Circulation*. 1977; 56:273–278. [PubMed: 872321]
15. Hoffmann R, von Bardeleben S, ten Cate F, Borges AC, Kasprzak J, Firsckhe C, Lafitte S, Al-Saadi N, Kuntz-Hehner S, Engelhardt M, Becher H, Vanoverschelde JL. Assessment of systolic left ventricular function: a multi-centre comparison of cineventriculography, cardiac magnetic

- resonance imaging, unenhanced and contrast-enhanced echocardiography. *Eur Heart J.* 2005; 26:607–616. [PubMed: 15618026]
16. Pearson JD, Morrell CH, Brant LJ, Landis PK, Fleg JL. Age-associated changes in blood pressure in a longitudinal study of healthy men and women. *J Gerontol A Biol Sci Med Sci.* 1997; 52:M177–M183. [PubMed: 9158560]
  17. Rademakers FE, Rogers WJ, Guier WH, Hutchins GM, Siu CO, Weisfeldt ML, Weiss JL, Shapiro EP. Relation of regional cross-fiber shortening to wall thickening in the intact heart. Three-dimensional strain analysis by NMR tagging. *Circulation.* 1994; 89:1174–1182. [PubMed: 8124804]
  18. Bogaert J, Rademakers FE. Regional nonuniformity of normal adult human left ventricle. *Am J Physiol Heart Circ Physiol.* 2001; 280:H610–H620. [PubMed: 11158958]
  19. Sengupta PP, Mohan JC, Mehta V, Jain V, Arora R, Pandian NG, Khandheria BK. Comparison of echocardiographic features of noncompaction of the left ventricle in adults versus idiopathic dilated cardiomyopathy in adults. *Am J Cardiol.* 2004; 94:389–391. [PubMed: 15276116]



### CLINICAL PERSPECTIVE

Whether an individual who has been found to have unusually prominent or extensive left ventricular (LV) trabeculations should be regarded as having pathological LV noncompaction has become a recurring dilemma for cardiologists and imaging specialists. This dilemma has arisen partly through improvements in imaging and partly through growing awareness of LV noncompaction as a possible pathological entity. Solution of the dilemma requires methodical study of normal ranges of image appearances to compare with those found in a patient by the same modality, and CMR often is the modality chosen to resolve the issue. The current study reports, for the first time, the segmental incidence of visible trabeculations and the segmental ranges of the thicknesses of the trabeculated relative to the compacted layers, as measured at end diastole and end systole in routine short-axis cine CMR in 120 healthy volunteers spanning 6 deciles of adult life. The measurements give novel insights into the prevalence, segmental distribution, dynamics, and likely functional role of the trabecular myocardial layer. The systolic thinning of the apparent trabeculated layer, in contrast to the marked thickening of the apparently compact myocardium, is discussed. It supports a functional role for trabecular rather than compact myocardial structure in certain endocardial regions and suggests, as others have previously, that changes associated with a dilated cardiomyopathy may in themselves lead to, and not necessarily result from, an abnormally high ratio of visibly trabeculated to compacted myocardial thickness.

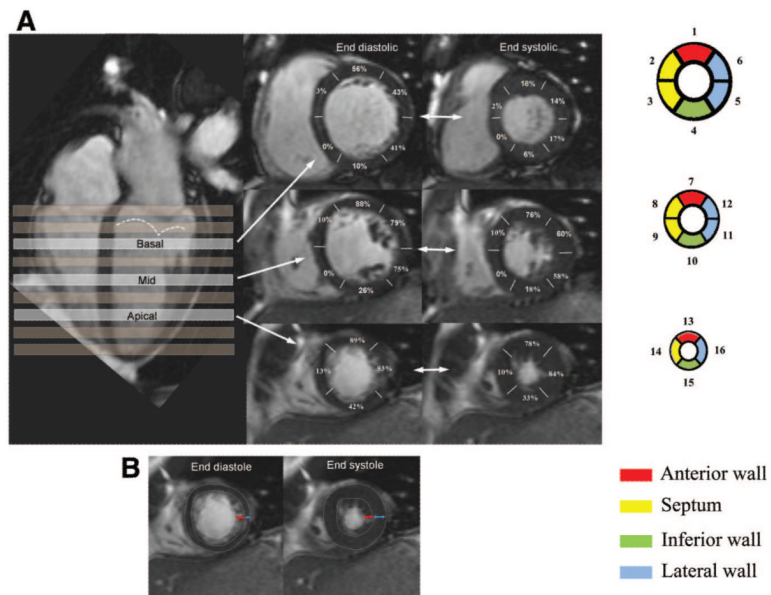


**Figure 1.** A, The systematic selection of basal, midcavity, and apical slices chosen for measurements of trabecular and compacted layer thickness is shown. The segmental incidence of apparent trabeculae seen at both ED and ES is indicated as percentages for each of the 16 segments. The dotted line indicates the ES location of the mitral valve. B, Examples of ED and ES frames showing the boundaries (dotted lines) of the trabeculated layer (red arrows) and compacted layer (blue arrows).

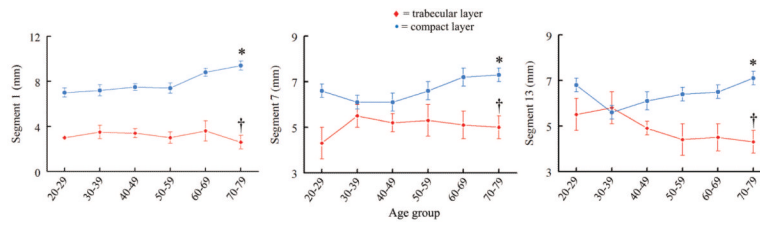


**Figure 2.**

Compacted and trabecular layer thicknesses at ED per age group (anterior wall). Data are plotted as mean $\pm$ SEM with the exception of the first data point representing the trabecular layer thickness in the 20 to 29 age group on segment 1, which is shown as median (first, third quartiles, 0, 4.6). \* $P$ <0.05 across age groups for the compacted layer. † $P$ <0.05 across age groups for the trabecular layer.

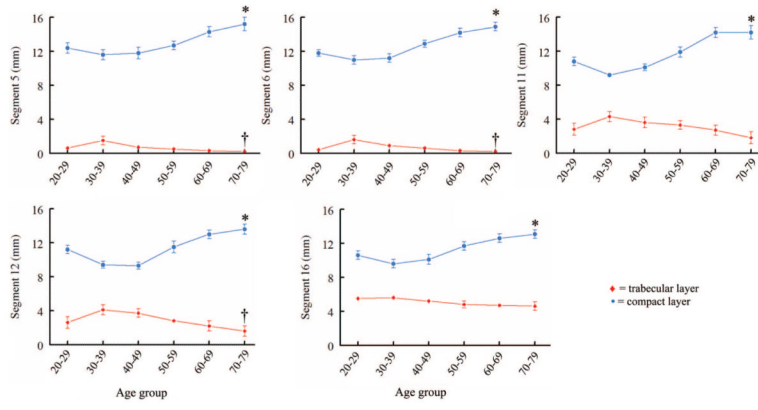


**Figure 3.** Compacted and trabecular layer thicknesses at ES per age group (lateral wall). Data are plotted as mean±SEM. \* $P < 0.05$  across age groups for the compacted layer. † $P < 0.05$  across age groups for the trabecular layer.

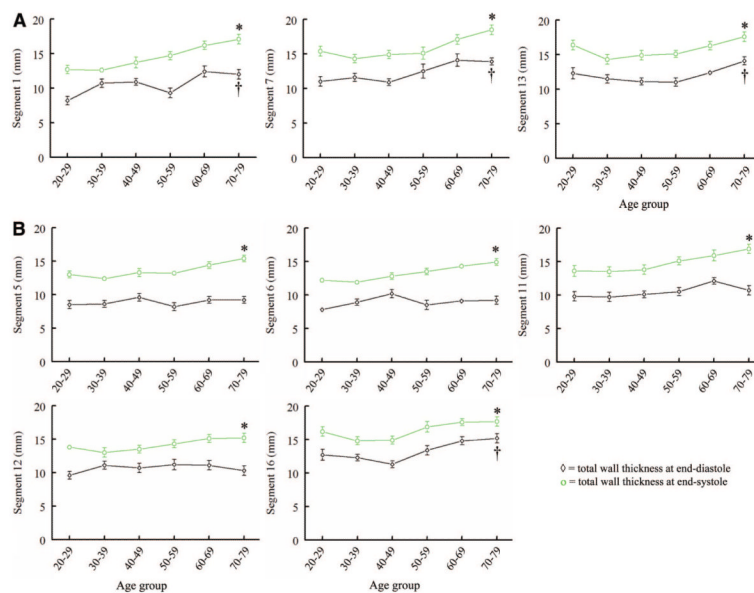


**Figure 4.** A, Total myocardial wall thickness (anterior wall) at ED and ES per age group. B, Total myocardial wall thickness (lateral wall) at ED and ES per age group. Data are plotted as mean±SEM. \* $P < 0.05$  across age groups for the total myocardial layer at ES. † $P < 0.05$  across age groups for the total myocardial layer at ED.

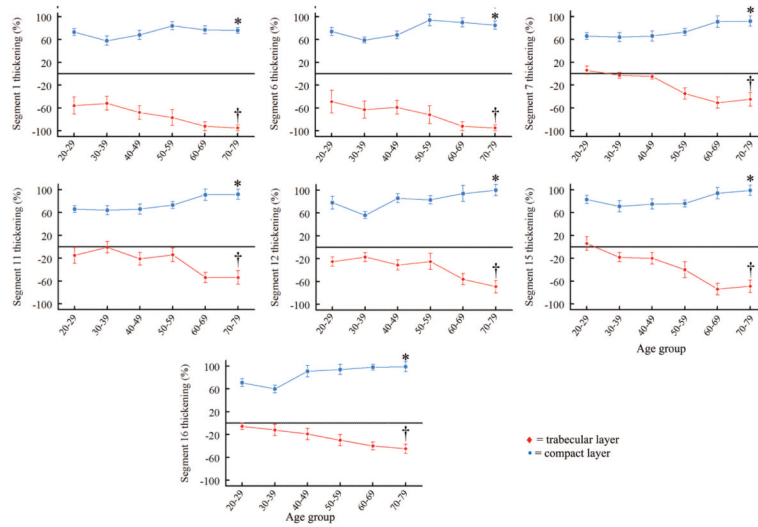


**Figure 5.** Systolic trabecular layer thinning and compacted layer thickening shown as a pattern with age in the most trabeculated LV segments. Data are plotted as mean±SEM. \* $P < 0.05$  across age groups for the compacted layer. † $P < 0.05$  across age groups for the trabecular layer.

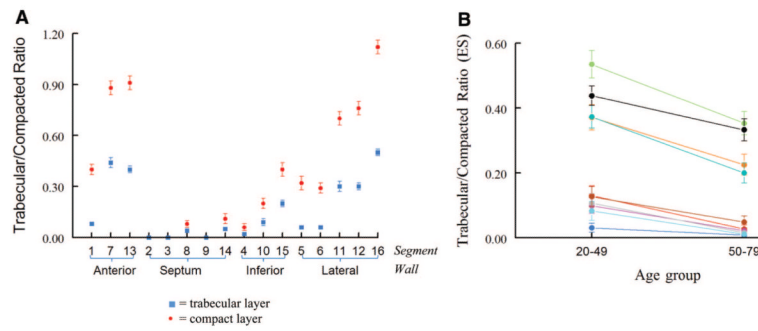


**Figure 6.** A, Trabecular/compacted ratio at ED (red) and ES (blue) in each segment. B, Trabecular/compacted ratio at ES in younger versus older patients in all 16 segments. Data are plotted as mean $\pm$ SEM. \* $P$ <0.05 in the young versus the old age group for each plotted segment.

**Table 1**

## Intra- and Interobserver Variability

	<b>Intraobserver Variability</b>	<b>Interobserver Variability</b>
Trabecular layer (diastole)	0.10±0.19	0.10±0.17
Trabecular layer (systole)	0.02±0.05	0.05±0.08
Compacted layer (diastole)	0.004±0.006	0.05±0.11
Compacted layer (systole)	0.02±0.08	0.02±0.09

Data are presented as mean±SD. Variability expressed as ratio between the difference and the mean of 2 independent readings.



Table 2

Thicknesses of Trabecular, Compacted, and Total Myocardial Layers at ED and ES and Thickening of Trabecular, Compacted, and Total Myocardial Layers

Segment	ED				ES				Wall Thickening*		
	Trabecular Layer, mm	Compacted Layer, mm	Total Wall, mm	Trabecular/Compacted Ratio	Trabecular Layer, mm	Compacted Layer, mm	Total Wall, mm	Trabecular/Compacted Ratio	Trabecular Layer, % <sup>†</sup>	Compacted Layer, %	Total Layer, %
1	3.0 (0, 4.6)	7.9±1.9	10.6±3.4	0.380±0.036 [1.6]	0	13.7±3.0	14.5±3.0	0.078±0.017 [0.9]	-30±10	72±13	43±13
2	0	9.6±2.5	9.6±2.5	0	0	14.0±2.8	14.0±2.8	0		49±12	46±12
3	0	8.7±2.0	8.6±2.0	0	0	11.7±2.4	11.7±2.4	0		34±12	31±13
4	0	7.7±1.7	8.0±2.1	0.059±0.018 [1]	0	13.1±2.5	13.2±2.7	0.019±0.007 [0.4]	-45±20	71±13	62±13
5	0 (0, 3.9)	7.0±1.6	8.9±2.4	0.318±0.044 [1.8]	0	13.0±2.5	13.6±2.4	0.060±0.013 [0.6]	-30±40	83±13	61±13
6	0 (0, 4.1)	7.0±1.4	9.0±2.5	0.289±0.034 [1.3]	0	12.7±2.6	13.2±2.3	0.061±0.015 [1]	-20±40	77±13	56±13
7	5.6±2.8	6.6±1.5	12.3±3.5	0.879±0.043 [2.2]	4.5±2.1	11.4±3.0	15.9±3.4	0.443±0.028 [1.7]	-20±40	75±13	34±12
8	0	7.9±1.6	8.4±1.9	0.080±0.025 [1.4]	0	12.9±2.9	13.3±2.8	0.046±0.015 [1.1]	-5±1	65±12	61±13
9	0	8.1±1.5	8.1±1.5	0	0	12.9±2.3	12.9±2.3	0		60±12	58±13
10	0 (0, 2.1)	7.1±1.4	8.4±2.4	0.203±0.035 [1.6]	0	12.3±2.9	13.2±3.1	0.088±0.018 [0.8]	-10±30	74±12	61±13
11	4.2±2.5	6.3±1.4	10.5±2.9	0.704±0.044 [1.8]	3.1±2.5	11.7±3.1	14.8±3.4	0.298±0.026 [1]	-26±40	87±13	84±15
12	4.4±2.7	6.3±1.4	10.7±2.9	0.756±0.048 [2.4]	2.8±2.1	11.3±2.8	14.1±2.9	0.287±0.024 [1]	-35±40	83±14	36±14
13	5.6±2.7	6.4±1.4	12.0±3.0	0.914±0.045 [2.2]	4.2±2.1	11.6±2.2	15.8±2.9	0.386±0.023 [1]	-16±40	87±13	36±12
14	0	7.3±1.7	8.0±2.5	0.112±0.031 [1.8]	0	12.7±2.4	13.1±2.4	0.046±0.014 [1]	-31±12	76±13	69±14
15	0 (0, 4.5)	6.1±1.4	8.3±2.6	0.395±0.046 [1.8]	0 (0, 3.6)	11.4±3.0	12.9±2.8	0.167±0.025 [0.8]	-32±30	85±13	63±14
16	7.1±2.4	6.1±1.3	13.2±3.3	1.190±0.042 [3]	5.0±2.3	11.2±2.7	16.3±3.1	0.493±0.025 [1.5]	-24±30	85±13	26±13
<b>Average all segments</b>		<b>7.4±1.5</b>	<b>9.7±2.5</b>			<b>12.4±2.7</b>	<b>14.0±2.6</b>		<b>-24±19</b>	<b>73±13</b>	<b>52±13</b>

Data are presented as mean±SD for normally distributed variables and as median (first, third interquartile ranges) for nonparametric variables. Data in brackets represent the highest ratio measured in each segment.

\* Calculated as [(ES-ED)×100]/ED.

<sup>†</sup> Minus implies thinning.